DOI: 10.12442/j.issn.1002-185X.20240455.

Effect of modification treatment and aging treatment on the microstructure-mechanical properties and electrical conductivity of an Al8Si0.4Mg0.4Fe alloy

Quanyi Xing [1, 2], Ge Zhou [1, 2], Haoyu Zhang [1, 2], Xin Che [1, 2], Wenjingzi Wang [1, 2], Lijia Chen [1, 2]

[1] School of Materials Science and Engineering, Shenyang University of Technology, Shenyang 110870, China; [2] Shenyang Key Laboratory of Advanced Structural Materials and Applications, Shenyang University of Technology, Shenyang 110870, China

Abstract: In this paper, self-designed Al8Si0.4Mg0.4Fe aluminium alloy was modified with Sr, and a solid solution + aging treatment was applied to the alloy to regulate its microstructure and properties. The results show that: after the modification treatment, the room temperature tensile strength of the alloy did not change much, the elongation at break slightly improved (1.82%→3.34%), and the electrical conductivity significantly increased from 40.1%IACS before the modification treatment to 42.0%IACS. After the modification, the alloy underwent a solid solution treatment at 515°C for 8 hours and subsequently an aging treatment at temperatures 180°C, 200°C, 220°C and 240°C for a duration of 6 hours. With the increase of aging temperature, the electrical conductivity increased monotonously from 41.4% IACS to 45.5% IACS, but the room temperature tensile strength increased first and then decreased. At 200℃, the electrical conductivity and room temperature tensile strength of the alloy showed a good coordination, the electrical conductivity was 42.5%IACS, and the room temperature tensile strength was 282.9MPa. When the aging temperature continues to rise, the alloy is overaged. Although the conductivity is still rising, the tensile strength at room temperature decreases sharply, and it is only 177.1MPa at 240℃.

Keywords: Al8Si0.4Mg0.4Fe alloy; electrical conductivity; aging treatment; room-temperature mechanical properties; microstructural evolution

Acknowledgement: This work was supported by the Applied Basic Research Program of Liaoning Province (CN) (No. 2022JH2/101300078).

About the author: Quanyi Xing, male, born in 1993, master, Shenyang University of Technology, Liaoning Shenyang, 110870, telephone number: 13940268381, e-mail: quanyi1022@163.com

Corresponding author： Ge Zhou, male, professor, Shenyang University of Technology, Liaoning Shenyang, 110870, telephone number: 18602408585, e-mail: zhouge@sut.edu.cn

Aluminium alloys are widely used in automotive manufacturing, construction, electronics, aerospace, power systems and many other fields due to their low density, high specific strength, good corrosion resistance and excellent electrical and thermal conductivity[1-3]. In particular, the electric power industry has gradually become the basic pillar industry for supporting the construction of China. In recent years, as the international community's call for energy savings and emission reduction has been increasing, the traditional power generation from thermal power generation to wind, hydro, and solar power generation has changed[4]. To better cooperate with the power system in the direction of energy saving and environmental protection transition, according to the international community's call for low-carbon environmental protection, in addition to changing the power generation method, how to reduce the loss of the power transmission process is an important direction of development in the future. Therefore, in the development of new power transmission conductors, ensuring that aluminium alloys have stable and reliable comprehensive mechanical properties while improving their electrical conductivity is an important factor in meeting the requirements of low energy consumption for new long-distance overhead conductors and large load-bearing components in the power transmission process (such as conductive parts of transmission switches and transmission components).

Casting aluminium -silicon alloys are widely used for structural parts with complex shapes in

power transmission systems due to their good casting ability and welding properties and low manufacturing costs[5]. Moreover, aluminium-silicon alloys have a small coefficient of linear expansion and are often used for parts that are required to maintain a high degree of dimensional accuracy under different temperature variations[6-8]. The Si phase of aluminium-silicon alloys, as the main reinforcing phase of these alloys, plays an important role in alloy design. First, the Si content is the key factor that directly affects the strength of aluminium-silicon alloys, and the strength of aluminium-silicon alloys will continue to increase with a continuous increase in the Si content; however, Si increases the scattering of electrons during the electron transport process, which results in a decrease in the plasticity and electrical conductivity of this alloy system[9-11]. To solve the above problems, researchers have used the idea of microalloying design, through the addition of alloying elements such as Mg, Cu, Ni, Fe and other alloying elements, to regulate the electrical conductivity and room temperature strength of aluminium-silicon alloys, and the results of the study show that[12] the presence of Mg can be formed in the aluminium-silicon alloy matrix of the Mg_2Si strengthened phase, and the formation of a small amount of the second phase is conducive to an increase in the thermal conductivity of the alloy, but with an increase in the Mg content, the alloy thermal conductivity increases. increases, the thermal conductivity of the alloy begins to gradually decrease[13,14]. A small amount of Fe will form a Chinese character-like α-AlFeSi phase or a needle-like β-AlFeSi phase in the matrix. These two phases have the metallic nature, and a uniform distribution in the matrix will have a promotional effect on the increase of the electrical conductivity. However, Ma Z et al., in a study of the effect of the Fe content on the fracture behaviour of Al-Si-Cu casting alloys, found that[15] the Fe content in aluminium-silicon alloys is greater than 0.5%, and the mechanical properties of the alloys will be sharply reduced; however, with increasing Mg content, the thermal conductivity begins to gradually decrease. The mechanical properties of the alloys decrease sharply. Therefore, the effect of the addition of different alloying elements on the electrical conductivity is due to the formation of second phases with different electrical conductivity coefficients and decreases with an increase in the number of second phases with low thermal conductivity[16]. On this basis, to achieve excellent property matching between the strength and electrical conductivity of aluminium-silicon alloys, scholars have attempted to further improve the comprehensive properties of these alloys by using the method of modification + heat treatment.

First, by adding Sr, Ni, Ce, Bi, Er and other elements as modifiers, eutectic Si is modified to form imperfect octahedra with primary dendrites or secondary dendrites after the modification treatment, which can significantly improve the strength and plasticity of the alloys[17-19]. Second, heat treatments are used to reduce defects in cast alloys and effectively regulate their microstructure; specifically, solid solution strengthening and second phase strengthening are the main mechanisms for increasing the strength of alloys during heat treatments, while nanoscale precipitates produced during artificial aging can significantly increase the electrical conductivity of alloys[20,21]. However, in general, aluminium-silicon alloys exhibit a decrease in electrical conductivity with increasing strength, and this phenomenon of inverted strength and electrical conductivity is currently a focus of much attention among scholars. Therefore, improving the electrical conductivity of the alloy as the primary goal through the design of the alloy system, the selection of suitable modifiers and the corresponding solid solution + aging treatment methods, on the basis of which to ensure that it has good room temperature mechanical properties, is particularly important for aluminium-silicon alloys.

For this reason, this paper considers the effect of several common alloying elements, such as Cu, Fe, and Mg, in Al-Si alloys from the point of view of the solid solubility of different alloying elements in Al-Si alloys with the generated second phase on the design of the alloys. Since the solid solubility of Fe in Al is very low, in the absence of precipitation of the Fe-containing second phase, it has the least influence on the electrical conductivity of the alloy, but due to its greater detrimental effect on the mechanical properties, the content of Fe should be less than 0.5%[16]. Cu and Mg have a large solid solubility in Al, and when they are dissolved in an aluminium matrix, the induced lattice distortions greatly increase the scattering of electrons, thus reducing the electrical conductivity[22]. It is worth noting that although the maximum solid solubility of Mg in Al is large, reaching 18.6 wt.%, at room temperature, it is only 1.2 wt.%, so it is possible to fully precipitate the supersaturated Mg atoms in the Al matrix by means of artificial aging and form Mg_2Si-strengthened phases with Si atoms in the microstructure, which is undoubtedly beneficial for enhancing the strength and electrical conductivity. Based on the above considerations, this study independently designed the Al8Si0.4Mg0.4Fe alloy, ingeniously utilizing Sr as a modifier to regulate the formation of finely fibrous eutectic silicon structures with rounded tips. With this

type of as-cast microstructure, experiments on the solid solution + aging heat treatment process were designed. Under the premise of fully exploiting the promoting effect of solid solution and aging treatments on enhancing electrical conductivity, we explored the influence of the size and quantity of the second phase on the electrical conductivity and ultimate tensile strength of the alloy. The aim is to obtain the optimal balance between strength and electrical conductivity for this alloy, and to reveal the influence mechanism of modification treatment and heat treatment processes on the microstructure, mechanical properties and electrical conductivity of the Al8Si0.4Mg0.4Fe alloy. This will provide solid theoretical support for expanding the practical application of this type of alloy.

1. Experiment

The experimental material is a self-designed AlSiMgFe alloy. According to the designed mass ratio, the raw material consists of industrial pure aluminium (99.7%), pure silicon (99.9%), industrial pure magnesium (99.9%), pure iron (99.9%), and Al-10Sr intermediate alloy. According to the designed alloy composition of the ingredients, the material is melted with a well-type melting furnace. First, pure aluminium was melted at 750°C, and then, pure silicon and pure iron were added to the molten aluminium solution. After all melted, pure Mg wrapped in aluminium foil was pressed into the bottom of the solution with a bell jar and gently stirred for 10 min. Then, a hexachloroethane refining agent was added, the mixture was gently stirred, the slag was skimmed off and left to stand for 10 min, the molten solution was poured into the moulds, which were preheated at 200°C, and the aluminium alloy ingots were obtained. The melting process for the modification treatment was consistent with that described above, and an Al-10Sr intermediate alloy was added before refining. Inductively coupled plasma optical emission spectrometry (ICP–OES) was used for alloy composition analysis, and the alloy composition (wt.%) is shown in Table 1.

Table 1 Chemical composition of the AlSiMgFe alloys

	Mg	Fe	Si	Sr	Al
Unmodified	0.453	0.423	8.16	/	Bal.
Modified	0.412	0.398	8.26	0.033	Bal.

The alloy was subjected to solid solution + aging treatment in a box-type resistance furnace with the following process parameters: solid solution temperature, 515°C; holding for 8 hours with water cooling; aging temperatures ranging from 180°C to 240°C with an interval of 20°C; and holding for 6 hours with air cooling. An Axio Observer Zeiss inverted metallurgical microscope (OM) was used to observe the microstructural changes before and after modification. The samples to be tested were polished step by step with 600#, 800#, 1000#, 1500#, 2000# sandpaper, and after roughly polishing the samples with 2.5 diamond abrasive paste, the samples were finely polished using a 0.05 alumina suspension. Subsequently, the samples were etched with 0.5% hydrofluoric acid solution for 10 s and then cleaned with anhydrous ethanol immediately after corrosion and blown dry. The room temperature mechanical property test specimens were processed using wire cutting in accordance with the dimensional specifications shown in Fig. 1, and tensile tests were carried out in an MTS Landmark 370.10 testing machine to obtain the values of the room temperature yield strength (YS), ultimate tensile strength (UTS) and elongation (EL) of the Al8Si0.4Mg0.4Fe alloy. Three samples were tested under each condition during the test process, and the results were averaged. A PZ-60A eddy current electrical conductivity meter was used to test the electrical conductivity of the alloy, five points in the same sample were selected for the experiment, and the results were averaged. After separately performing surface treatments on the samples before and after the modification treatment, the phase composition in the microstructure was analysed using an XRD-7000 X-ray diffractometer (XRD). The parameters of the XRD experiment were as follows: the target material was Cu, the working voltage was 40 kV, the scanning angle was 20°-90°, and the scanning speed was 4°/min. Backscattered electron imaging with a SU8020 scanning electron microscope (SEM) was used to observe the second phase composition in the microstructure as well as the morphology of the tensile fracture surface.

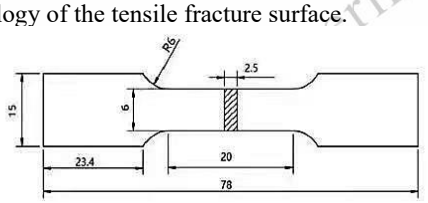

Fig. 1. Dimensions of the tensile specimen

2. Results and analyses

2.1 Effect of the modification treatment on the microstructure

The morphology of the as-cast aluminium-silicon alloys before and after modification is shown in Fig. 2(a) and 2(b). An α-Al matrix and coarse lamellar eutectic silicon can be clearly observed in the unmodified alloy, and the lamellar eutectic silicon is randomly and haphazardly distributed in the matrix. The eutectic silicon phase in the alloy microstructure

after Sr modification underwent obvious changes, from plate-like to the tip of the rounded and small fibrous transformation, while the α-Al phase in the microstructure exhibited an obvious rounded area, and the contact interface with the silicon phase became smooth and flat. This is due to the low solubility of Sr in Al, as the alloy melts during the solidification process, and Sr will be free in the liquid–solid interface front. When the eutectic temperature is reached, the eutectic Al-Si begins to grow in the interdendritic spaces of the α-Al dendrites. Concurrently, the Sr atoms that are free in the liquid phase are enriched at the front end of growth, inhibiting the growth rate of eutectic Si, and at the same time, the adsorption of Sr atoms onto the growth steps of Si leads to a change in the direction of growth of the eutectic Si. The growth direction changes, thus making the eutectic Si fibrous, which is consistent with the findings of Jenkinson D. C. et al.[23]. To determine whether the phase composition of the alloy changed after modification, XRD tests were carried out on the alloy before and after modification, and the results of the tests are shown in Fig. 2(c), which shows that no new phases were generated in the modified alloy, and the as-cast alloy microstructure mainly consisted of the α-Al matrix, the eutectic Si phase, and a small amount of the AlFeSi phase and the Mg_2Si phase.

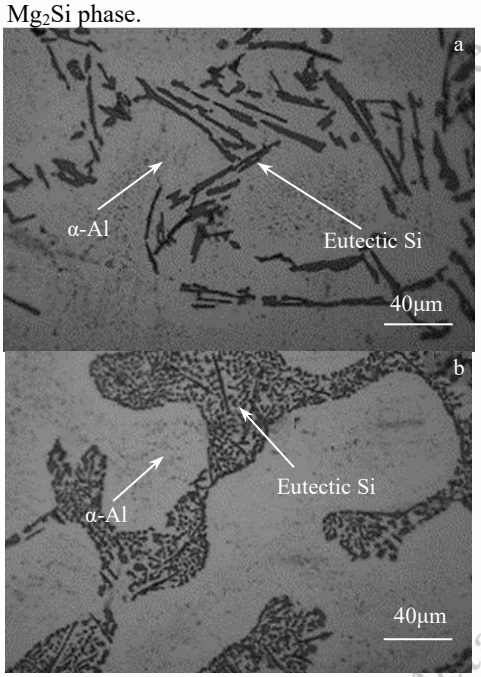

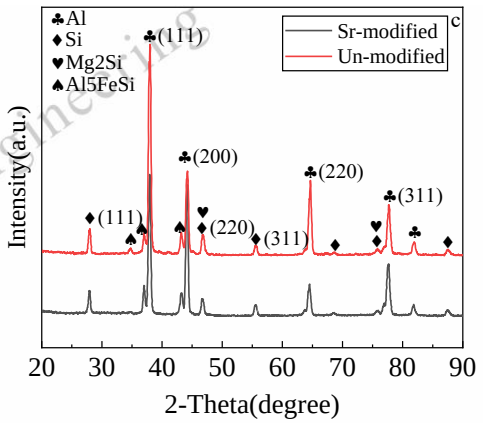

Fig. 2 Microstructure and XRD patterns of the alloy before and after modification: (a) unmodified, (b) modified, and (c) XRD pattern

Figure 3(a) shows the SEM image of the AlSiMgFe alloy after modification, and it can be seen that there are three main reinforcing phases in the alloy microstructure. In addition to the eutectic silicon phase, which can be clearly distinguished, the other two phases were analysed by energy spectroscopy and can be seen at points A and B in Figure 3(a). The elemental composition of point A is Al, Fe, and Si, which can be identified as the β-AlFeSi phase by combining with its long needle-like morphology. The energy spectrum of point B shows that Al, Mg, and Si are present at this point, and at the same time, the atomic ratio of Mg to Si is close to 2:1. Based on the XRD analysis results, It can be inferred that the black secondary phases exhibiting clustered distributions are identified as Mg2Si phases. The maximum solubility of Mg in Al is 18.6%, but at room temperature, the solid solubility of Mg in Al is only 1.2%, and when the content of Mg exceeds the solid solubility, it precipitates out of the Al matrix and combines with Si atoms in the microstructure to form the Mg_2Si phase. The solubility of Fe in Al is extremely low, and thus, during solidification, nearly all the Fe atoms in the alloy composition fail to dissolve into the aluminium matrix. Instead, they exist in the matrix as iron-rich secondary phases. In addition to exhibiting the long needle-like morphology at point A in Figure 3(a), it also exists in the aluminium-silicon alloy in the form of a Chinese character-like morphology. However, due to its poor stability, its content is relatively low and has not been detected in the microstructure of this alloy.

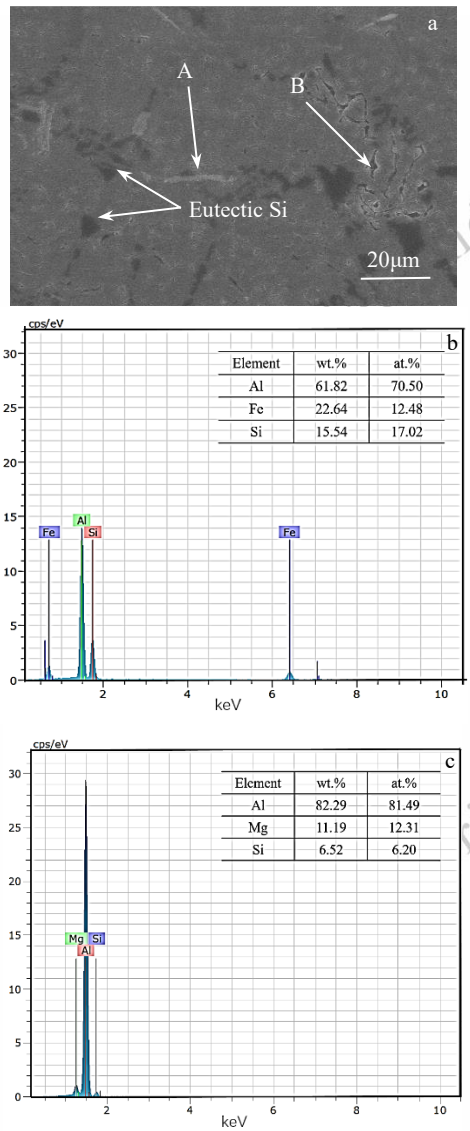

Fig. 3 SEM morphology and EDS energy spectrum of the modified alloy: (a) SEM image, (b) EDS image at point A, and (c) EDS image at point B.

2.2 Effect of modification treatment on electrical conductivity

Figure 4 shows a schematic diagram of electron movement in monatomic and polyatomic systems. After the modification treatment, the electrical conductivity of the as-cast aluminium-silicon alloy increases from 40.1%ICAS to 42.0%ICAS. This is due to the change in the morphology of the eutectic silicon, which leads to a reduction in the obstruction of the electron transport process, and the scattering effect experienced by free electrons in the alloy matrix is diminished. For the monoatomic system, the electrons undergo transitions from a lower energy level to a higher energy level when they gain energy, thus leaving holes in the positions where the electrons were originally located, as shown in Fig. 4(a). In polyatomic systems, upon gaining energy, electrons can undergo tunneling transitions from one atom to another nearby atom[24]. Concurrently, subsequent electrons will also undergo similar transitions to occupy the positions previously held by those electrons, thereby initiating the conduction of electrons in the conductor, as depicted in Figures 4(b) and 4(c). As silicon (Si) is a semiconductor, the binding energy of Si atoms to electrons is relatively strong, resulting in a larger energy requirement for electron transitions. Since there are no vacancies in the lower energy levels of its electrons, it is difficult for other electrons to enter these levels. Therefore, the electrical conductivity of the Si phase is significantly weaker than that of metals. Figure 5 shows a schematic diagram of electron transport in the Al-Si alloy system. In Al-Si alloys, the Si phase is the main obstacle in the electron transport process, and the free electrons in Al are more inclined to move directionally around the Si phase. According to classical electron theory, the resistivity of a conductor is directly proportional to the scattering coefficient of electrons in the conductor and inversely proportional to the mean free path of electrons. After the modification treatment, the contact area between the eutectic Si phase and α-Al in the alloy increases, which also enlarges the gaps between eutectic silicon particles, leading to an increase in the mean free path of free electrons. This results in an improvement in the electrical conductivity of the aluminium-silicon alloy.

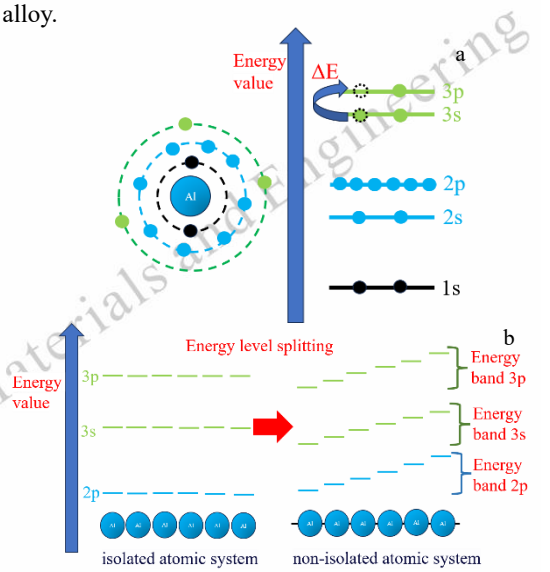

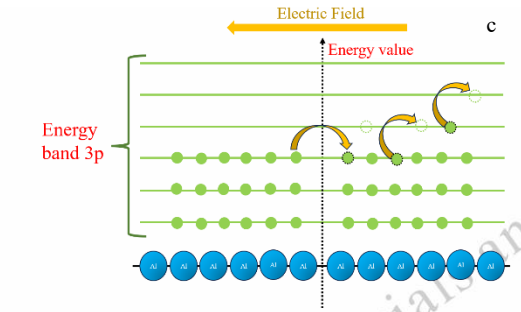

Fig. 4 Schematic diagram of electron movement: (a) Monatomic system, (b) energy level splitting in polyatomic system, (c) polyatomic system

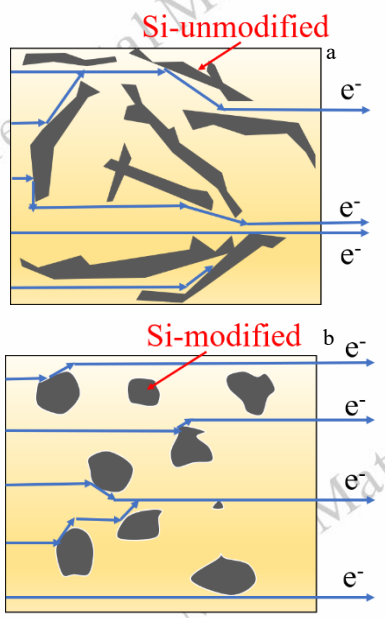

Fig. 5 Schematic diagram of electron transport before and after modification: (a) unmodified and (b) modified samples

2.3 Effect of modification treatment on the mechanical properties

Figure 6 shows the experimental results of the tensile strength of the aluminium-silicon alloy before and after modification. The ultimate tensile strength of the alloy did not change significantly after the modification treatment, but its elongation at break significantly improved from 1.82% to 3.34%. In this alloy, the eutectic silicon phase has the largest number and largest size, and it is the main reinforcing phase affecting the strength and plasticity of the alloy. After the modification treatment, the growth mode of eutectic silicon changed, and the change in its morphology and the reduction in its size reduced the fragmentation effect on the matrix, which led to a significant increase in the elongation at break. After the addition of the Sr modifier, the crystallization range of the alloy increased due to the inhibition of Si growth by the Sr, and the incipient α-Al grew into coarse dendrite structures, as shown in Fig. 2(b), which in turn induced a certain change in the fracture mode of the alloy. As seen from the tensile fracture morphology before and after the modification treatment shown in Fig. 7, the fracture morphology of the as-cast aluminium-silicon alloy without modification treatment shows a large number of cleavage planes, which is typical of brittle fracture characteristics. In the modified aluminium-silicon alloy, a small number of dimples appeared near the cleavage planes, which showed quasi-cleavage fracture characteristics. The α-Al matrix grew sufficiently, and the size of the eutectic silicon decreased, which was the reason for the slight decrease in the ultimate tensile strength and yield strength of the alloy.

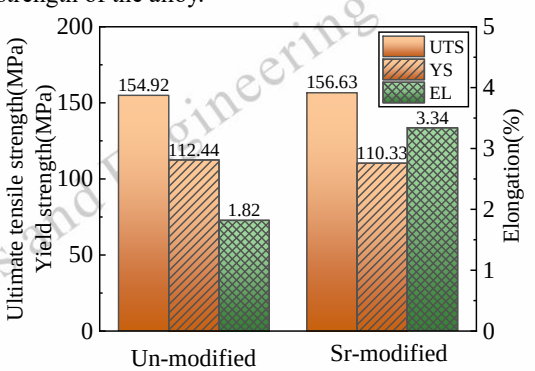

Fig. 6 Mechanical properties of alloys before and after modification treatment

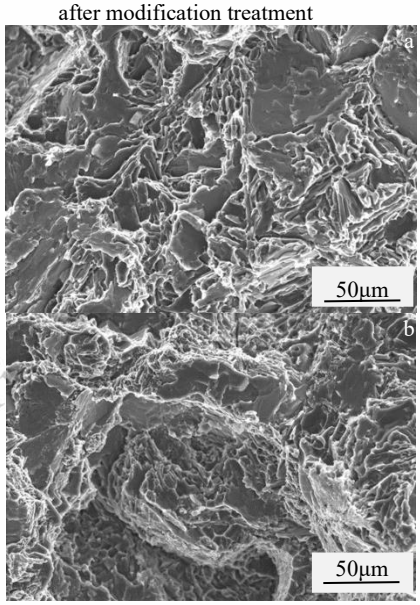

Fig. 7 Tensile fracture morphology of the (a) unmodified and (b) modified alloys before and after modification

Therefore, after the Sr modification treatment, the morphology of the eutectic silicon in the alloy microstructure effectively changed, resulting in an increase in the electrical conductivity and elongation at break of the alloy. However, the effect of the modification treatment on other reinforcing phases in the alloy is small, and the ultimate tensile strength of the alloy remains low. The supersaturated Mg atoms solidly dissolved in the α-Al matrix during solidification of the alloy could not be precipitated by means of the modification treatment. Therefore, the solid solution + aging treatment is used to further purify the matrix and reduce the lattice distortion of the α-Al matrix so that the solid-solved atoms can precipitate out sufficiently and uniformly, and the alloy can be further strengthened by the formation of a dispersed distributed second phase.

2.4 Effect of aging temperature on the microstructure

Figure 8 shows the microstructure of the alloy after aging at different temperatures. After the solid solution + aging treatment, the eutectic silicon phase in the modified alloy underwent obvious spheroidization, and the large eutectic silicon phase fused during the heat treatment process, splitting into finer eutectic silicon particles, which decreased the average size of the eutectic silicon phase and increased the number of particles. The size and morphology of the β-AlFeSi phase did not change significantly, and it was still distributed randomly and haphazardly in the matrix in the form of long needles. in the form of long needles, which are still randomly and haphazardly distributed in the matrix.

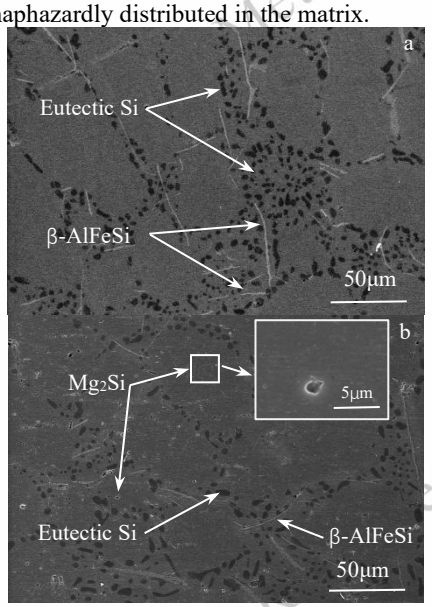

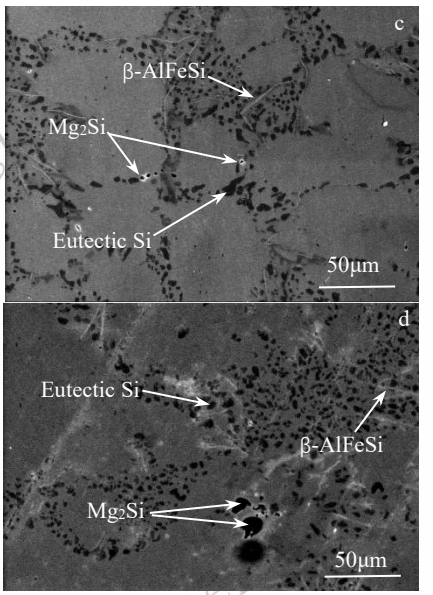

Fig. 8 SEM morphology of the alloy at different aging temperatures: (a) 180°C, (b) 200°C, (c) 220°C, and (d) 240°C

As the aging treatment temperature increases, the Mg_2Si phase in the alloy gradually increases, and its size also increases. As shown in Fig. 8. The precipitated Mg_2Si phase was not observed in the aluminium-silicon alloy microstructure at an aging temperature of 180°C, which indicates that at this temperature, all the Mg is dissolved in the matrix after solid solution treatment, and at 180°C, it is not enough for the Mg to precipitate out of the matrix. However, when the aging temperature was increased to 200°C, very fine Mg_2Si particles could be observed in the matrix and were dispersed in the matrix. When the aging temperature continues to increase, the Mg_2Si phase in the microstructure starts to increase, the size continues to increase, reaching approximately 3 μm at 220°C, and an overaging phenomenon starts to occur. By 240°C, the size reached 10 μm.

During the aging process, in addition to the changes in the morphology and quantity of the larger second phases in the alloy microstructure, more fine nanoscale precipitates will also form inside these second phases, which will have a positive impact on the electrical conductivity and mechanical properties of the alloy[25]. As shown in Figure 9a, these fine nanoscale precipitates are distributed at the interface between the matrix and the second phase in large quantities and appear as spherical particles. In order to determine the composition of these phases, energy spectrum analysis was performed on points A, B, and C in Figure 9a, and the results are shown in Figures 9b, 9c, and 9d. It can be seen that point A in the figure is the Al matrix, while the second phase that serves as

the carrier of nanoscale precipitates is the eutectic Si phase. The composition of these fine nanoscale precipitates includes Al and Si elements. Since eutectic silicon serves as the substrate of these black particles and its size is too small, the presence of Si elements cannot be avoided during the analysis. Therefore, it can be inferred that these nanoscale precipitates are spherical particles of Al, which is consistent with the research results of Xi H H et al.[26]. It is precisely due to the presence of these nanoscale Al particles that the local free electron density is increased, and the fracture tendency of the Si phase is reduced, which will also play a certain role in promoting the improvement of electrical conductivity and strength.

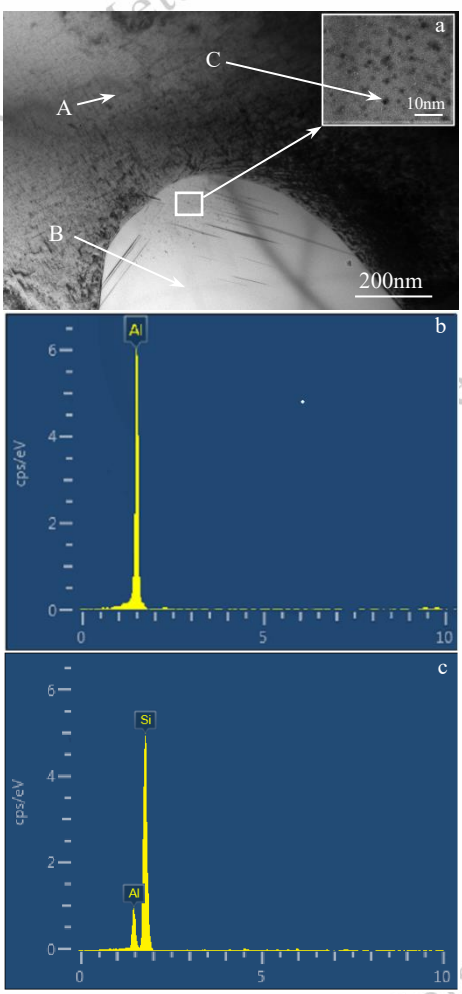

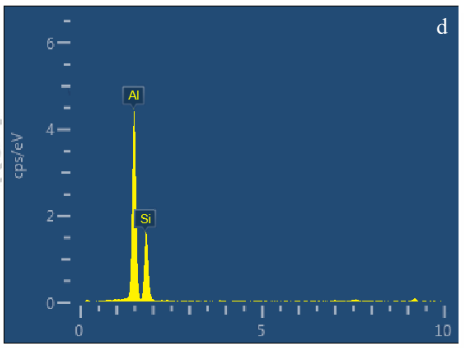

Fig. 9 TEM morphology of nanoscale precipitates and EDS energy spectrum: (a) TEM image, (b) EDS image at point A, (c) EDS image at point B, and (d) EDS image at point C

2.5 Effect of aging temperature on the electrical conductivity

Figure 10 shows the electrical conductivity of the alloy at different aging temperatures. As the aging temperature increases, the electrical conductivity of the alloy increases and finally plateaus. At 180°C, all the Mg atoms and a small amount of Si atoms are dissolved in the α-Al matrix, which reduces the purity of the Al matrix and decreases the free electron density in the matrix, and at the same time, due to the increase in the defect density in the Al matrix, the lattice distortion in the crystals increases, resulting in a decrease in the mean free range of electrons, which leads to a decrease in the electrical conductivity of the alloy. At 200°C, Mg begins to precipitate in the Al matrix, and due to the strong binding ability of Mg and Si, the precipitated Mg atoms combine with Si atoms to form the Mg_2Si phase. Mg_2Si and Si are both semiconductors, but the electrical conductivity of Mg_2Si is much stronger than that of Si[23], and the precipitated Mg atoms consume a part of the electrical conductivity during the formation of the second phase of Mg_2Si in the microstructure. The eutectic Si phase with poorer electrical conductivity is consumed by the precipitated Mg atoms, while the α-Al matrix is purified, resulting in an increase in the electrical conductivity of the alloy. As the aging temperature continues to increase, the alloy begins to experience over-aging phenomena. The Mg_2Si phase precipitated in the alloy microstructure starts to gather and grow. The Al matrix is the main channel for electron transport, the growth of this second phase is less of an obstacle to electron transport, and the number of main channels in the process of electron transport does not undergo any major change, so the electrical conductivity of the alloy changes less at temperatures higher than 220°C.

The eutectic Si phase becomes more rounded after heat treatment, and the large Si phase undergoes

disintegration to form fine Si particles, with increased interstitial space between the Si particles and increased channels for electron transport, resulting in a slight increase in electrical conductivity.

After solid solution treatment and aging at different temperatures, the morphological size and quantity of the Fe-rich phase did not significantly change. The solubility of Fe in Al is very low or even negligible. The Fe in the composition of this alloy exists in the form of an Fe-rich second phase in the alloy microstructure, most of which forms the β-AlFeSi phase, and a very small amount of Fe forms the α-AlFeSi phase. Due to the low content of α-AlFeSi, it was not observed in this alloy microstructure. The β-AlFeSi phase present in these microstructures is metallic and has a small effect on the electrical conductivity[27]. The presence of Fe consumes a portion of the Si atoms in the alloy with poor electrical conductivity and reduces the amount of Si phase in the disguise, which has a certain promotion effect on the electrical conductivity of the alloy. This promoting effect is equivalent at different aging temperatures, and the change in the electrical conductivity of the alloy is mainly due to the number and size of the Mg_2Si phase and the purity of the α-Al matrix.

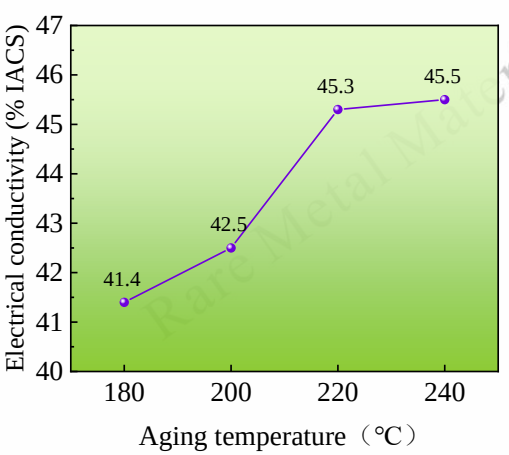

Fig. 10 Electrical conductivity of alloys at different aging temperatures

2.6 Effect of aging temperature on alloy strength

Figure 11(a) shows the stress–strain curves of tensile tests at different aging temperatures. The UTS of the alloy increases and then decreases with increasing temperature, reaching a maximum value of 282.9 MPa at 200°C, as shown in Fig. 11(b). At 180°C, Mg atoms and a small amount of Si atoms were solidly dissolved in the matrix, the lattice distortion of the matrix increased, and the resistance of dislocation movement in the matrix increased, resulting in solid solution strengthening. At the same time, the large eutectic Si particles are refined and spheroidized, the roundness of the Si particles increases, and these refined eutectic Si particles become more dispersed than before heat treatment, resulting in increased dispersion strengthening. The simultaneous existence of these two main strengthening modes results in a substantial increase in the tensile strength of the alloy compared to that of the as-cast state. When the potentiometric temperature is 200°C, the Mg and Si atoms that are solidly dissolved in the α-Al matrix begin to precipitate and form a dispersed fine Mg_2Si phase, as shown in Fig. 8(b). Due to the small size difference between the Mg and Al atoms, the lattice distortion produced during the formation of the replacement solid solution is also small, and the second-phase strengthening effect produced when the Mg atoms precipitate from the solid solution is much greater than that of solid solution strengthening, which leads to a further increase in the tensile strength of the alloy. When the temperature continues to increase, the dispersed Mg_2Si phase begins to aggregate and grow, and the dispersion strengthening effect is weakened. Moreover, the size of the eutectic Si phase increases, and the roundness begins to decrease, thus leading to a decrease in the strength of the alloy. From the fracture morphology of the tensile specimens of the alloy under different heat treatment conditions (Fig. 12), it can be seen that with increasing aging temperature, the dimples in the fracture morphology of the alloy tensile specimens gradually increase, and the cleavage effect on the matrix is weakened due to the tip passivation and spheroidization produced by the brittle eutectic Si phase, which gradually decreases the cleavage plane area of the alloy. When the aging temperature reached 220°C, the Mg_2Si phase dispersed in the matrix aggregated and grew, as shown in Figs. 8(c) and 8(d), and the decreased resistance to dislocation movement in the α-Al matrix enables the plasticity of the Al matrix to be expressed, leading to a significant increase in the number of dimples in the tensile fracture surface, which results in a decrease in the alloy's strength but an increase in its plasticity. Although the β-AlFeSi phase has a high hardness, it exists in the matrix in the form of long needles, and it is not possible to change its morphology by means of heat treatment. This morphology produces a cleavage effect on the matrix, which is very disadvantageous to the mechanical properties of aluminium-silicon alloys. However, the β-AlFeSi phase has metallic characteristics in terms of electrical conductivity[28,29], and when it is uniformly distributed in an aluminium matrix, it has virtually no effect on the electrical conductivity of the

alloy. At the same time, due to the presence of a small amount of the AlFeSi ternary phase, the content of the Si phase in the alloy decreases, which leads to a slight increase in the electrical conductivity of aluminium-silicon alloys.

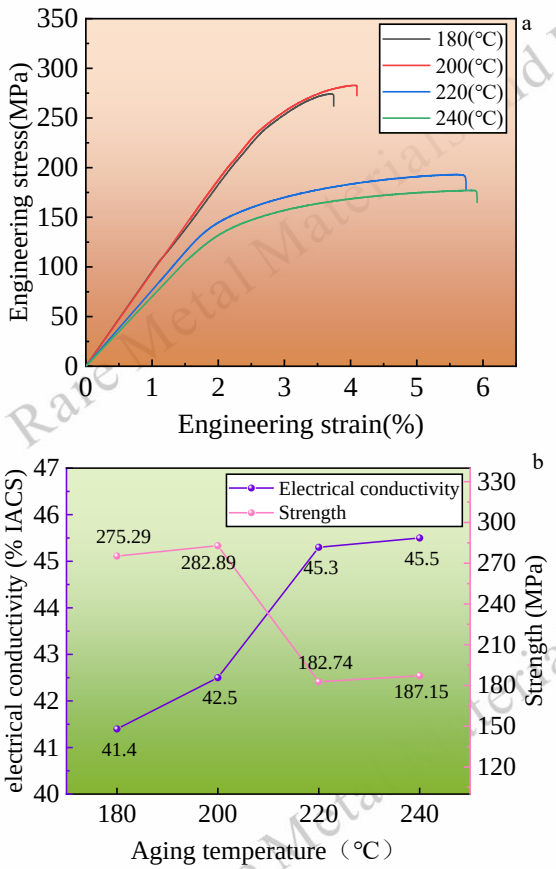

Fig. 11 Tensile curves and UTS and EC at different ageing temperatures: (a) tensile curves and (b) UTS and EC

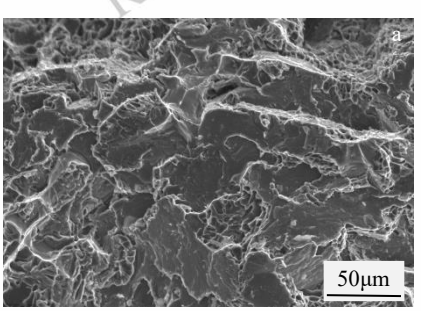

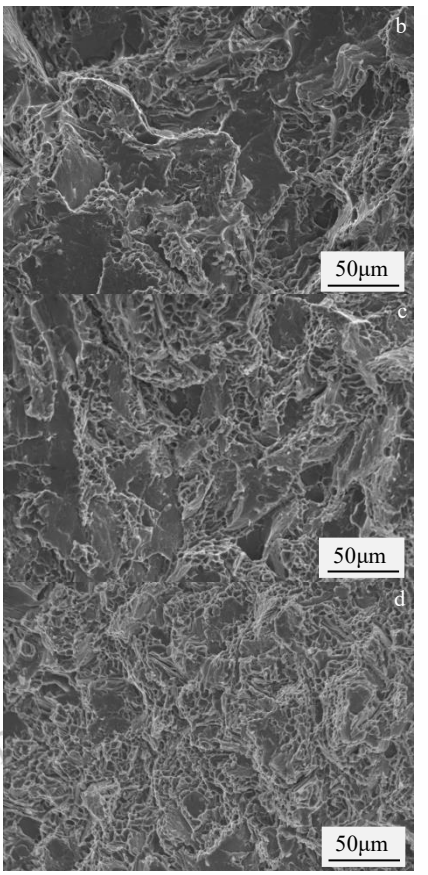

Fig. 12 Tensile fracture morphology at different aging temperatures: (a) 180°C, (b) 200°C, (c) 220°C, and (d) 240°C

3. Conclusions

In this paper, the microstructure and properties of a self-developed Al8Si0.4Mg0.4Fe alloy were modulated by using Sr modification treatment and heat treatment. The following important results were achieved:

1. After the modification treatment, due to the change in the morphology of the eutectic silicon phase of the microstructure, which reduces the scattering effect on the electrons, the electrical conductivity of the alloy is significantly improved, with the original 40.1%IACS increasing to 42.0%IACS, the tensile strength of the alloy is not significantly improved, the fibrous eutectic silicon has a weakened fragmentation effect on the substrate compared to the plate-like eutectic silicon, and the plasticity has improved from 1.82% to 3.34%.

2. The modified alloy was subjected to solution treatment at 515°C and aging treatment at 200°C to achieve simultaneous increases in electrical conductivity and strength. The Mg atoms solidly dissolved in the α-Al matrix precipitated uniformly

during the aging process and formed a fine and dispersed Mg_2Si phase with Si atoms. The α-Al matrix was sufficiently purified, the electrical conductivity of the alloy increased to 42.3%IACS, and the dispersion strengthening effect produced by the Mg atoms in the second phase was much greater than that of the solid in the matrix, and the obstruction of dislocation motion increased. The tensile strength increased to 282.9 MPa, but the elongation at break decreased from 3.34% to 1.83%.

3. Under the combined effect of modification and heat treatment, the morphology and quantity of the eutectic silicon and Mg_2Si phases in the alloy structure undergo significant changes, and these changes in the second phase distinctly alter the electrical conductivity of the alloy. This demonstrates that the conductivity and strength of the Al8Si0.4Mg0.4Fe alloy can be enhanced concurrently through a combination of modification and heat treatment.

Acknowledgement

This work was supported by the Applied Basic Research Program of Liaoning Province (CN) (No. 2022JH2/101300078).

Conflict of interest

On behalf of all authors, the corresponding author states that there is no conflict of interest.

Data availability

The datasets generated during and/or analysed during the current study are available from the corresponding author on reasonable request.

References

1 Sahoo B,Das T,Paul J *et al. Surface review and letters*[J],2022,29(9):1
2 Sang Kyu Y,Ji Won K,Myung Hoon O et al.Materials[J],2022,15(17):6103
3 Chen W H,Liu F C,Niu P L *et al. Rare Metal Materials and Engineering*[J],2024,53(4):1111 (in Chinese)
4 Tayeb M,Frida G C,Jose R *et al.IEEE Power and Energy Magazine*[J],2019,17(3):22
5 Esmeralda A,Arenas-García H,Rodríguez A *et al.Thermochimica Acta*[J],2019,675:172
6 Callegari B,Lima N T,Coelho S R.*Metals*[J],2023,13(7):1174.
7 Haghayeghi R,Timelli G.*Materials Letters*[J],2021,283:128779
8 Toshio H,Shinjiro I,Hiroshi F.Materials[J],2021,14(18):5372
9 Chen J K,Hung H Y,Wang C F *et al.Journal of Materials Science*[J],2015,50:5630
10 Wu L,He B,Li W *et al.Journal of Physics: Conference Series*[J],2021,2133(1):012021
11 Wang Y,Liao H,Wu Y *et al.Materials & Design*[J],2014,53:634
12 Li X, Cui X, Liu H *et al.Journal of Materials Science*[J],2023,58:8478
13 Kimura T,Nakamoto T,Ozaki T *et al.Materials Science and Engineering: A*[J],2019,754:786
14 Guo W C,Chen X H,Liu P *et al.Advanced Engineering Materials*[J],2021,23(3):2000955
15 Ma Z,Samuel A M,Doty H W *et al.Materials & Design*[J],2014,57:366
16 Stadler F,Antrekowitsch H,Fragner W *et al.Materials Science and Engineering: A*[J],2013,560:481
17 Zhang J,Zhou Y P,Sun C C *et al.Materials Science Forum*[J],2020,993:12
18 Li Y X,Fu Y T,Nie X *et al.Key Engineering Materials*[J],2022,921:3
19 Fang W Q,Shen J R,Yan J K et al. *Rare Metal Materials and Engineering*[J],2023,52(07): 2326
20 Yu W B,Zhao H B,Wang L *et al.Journal of Alloys and Compounds*[J],2018,731:444
21 Hou J P,Wang Q,Zhang Z J *et al.Materials & Design*[J],2017,132:148
22 Kim C W,Cho J I,Choi S W *et al.Advanced Materials Research*[J],2013,813:175
23 Jenkinson D C,Hogan L M.*Journal of Crystal Growth*[J],1975,28(2):171
24 Wei D.*Solid state physics*[M], Tsinghua University,Beijing, 2007
25 Hou J P,Wang Q,Zhang Z J *et al.Materials & Design*[J],2017,132:148
26 Xi H H,Ming W Q,He Y *et al.Journal of Alloys and Compounds*[J],2022,906:164238
27 Fang C M,Que Z P,Fan Z.*Journal of Solid State Chemistry*[J],2021,299:122199
28 Allamki A,Al-Maharbi A,Qamar S Z et al.*Metals*[J],2023,13(6):1111
29 Kim J M,Yun H S,Park J S *et al.International Journal of Cast Metals Research*[J],2013,27(3):141

变质处理和时效处理对 Al8Si0.4Mg0.4Fe 合金组织-力学性能及其电导率的影响

邢全义[1,2]，周舸[1,2]，张浩宇[1,2]，车欣[1,2]，王文静子[1,2]，陈立佳[1,2]

(1. 沈阳工业大学 材料科学与工程学院，辽宁 沈阳 110870)

(2. 沈阳工业大学 沈阳市先进结构材料与应用重点实验室，辽宁 沈阳 110870)

摘 要：本文对自主设计的 Al8Si0.4Mg0.4Fe 铝合金进行了 Sr 变质处理及固溶+时效处理，以调节其组织和性能。结果表明：变质处理后，合金的室温抗拉强度变化不大，断裂伸长率略有提高（1.82%→3.34%），电导率由变质处理

前的 40.1%IACS 显著提高到 42.0%IACS。将变质处理后的合金在 515℃固溶处理 8h，然后在 180℃、200℃、220℃和 240℃时效处理 6h。随着时效温度的升高，材料的电导率由 41.4%IACS 单调增加到 45.5%IACS，室温拉伸强度先升高后降低。在 200℃时，合金的电导率与室温拉伸强度表现出良好的协调性，电导率为 42.5%IACS，室温拉伸强度为 282.9MPa。当时效温度继续升高时，合金产生过时效现象。虽然电导率仍在上升，但室温拉伸强度急剧下降，在时效温度 240℃时仅为 177.1MPa。
关键词：Al8Si0.4Mg0.4Fe 合金; 电导率; 时效处理; 室温力学性能; 显微组织演变

作者简介：邢全义，男，1993 年生，硕士，沈阳工业大学材料科学与工程学院，辽宁 沈阳 110870，E-mail：quanyi1022@163.com
通讯作者：周舸，男，博士，教授，沈阳工业大学材料科学与工程学院，辽宁 沈阳 110870，E-mail：zhouge@sut.edu.cn